

# Modulating Electronic Interactions between Closely Spaced Complementary $\pi$ Surfaces with Different Outcomes: Regio- and Diastereomerically Pure Subphthalocyanine- $C_{60}$ Tris Adducts\*\*

David González-Rodríguez, Esther Carbonell, Dirk M. Guldi,\* and Tomás Torres\*

The operation of many emerging organic/plastic optoelectronic technologies,<sup>[1]</sup> such as solar-energy conversion devices,<sup>[2]</sup> relies ultimately on the ground- and excited-state electronic interactions between donor (D) and acceptor (A) components. The need to understand and control the primary photophysical events occurring within the active layers, as nature illustrates in the photosynthetic reaction center,<sup>[3]</sup> has prompted chemists to design and study molecular D–A models. In these, the yields and kinetics of energy and/or electron transfer are related to the nature of the D and A components<sup>[4]</sup> and their relative distance,<sup>[5]</sup> orientation,<sup>[6]</sup> or electronic coupling.<sup>[7]</sup> Importantly, the knowledge gathered so far has led to discrete molecular systems with improved charge-separation performance in solution.<sup>[8]</sup> However, most of these D–A models fail to reproduce a major characteristic of solid-state devices: molecules are usually confined by intimate van der Waals contacts, and conformational or orientational motion is restricted. Natural photosynthetic systems already demonstrate the importance of orbital overlap between embedded chromophores. In the so-called special pair, for instance, strong electronic coupling between two chlorophyll molecules held in close  $\pi$ – $\pi$  contact causes a red shift in the absorption that acts as a sink for all the energy collected.<sup>[3,9]</sup>

Herein we report a model system in which a D–A pair is forced to strongly interact through their  $\pi$  surfaces in a very rigid and closely spaced structure.<sup>[10]</sup> We demonstrate how small alterations in the distance between the two  $\pi$  surfaces, and therefore in the degree of orbital overlap and electronic coupling, influence the ground- and excited-state interactions. To maximize the contact area, we exploited the complementarity between the concave aromatic surface of subphthalocyanines (SubPcs),<sup>[11]</sup> versatile chromophores that have shown outstanding, tunable properties in D–A systems,<sup>[12]</sup> and  $C_{60}$ .<sup>[13]</sup> At the same time, in order to hold the two units in close contact and to limit the flexibility of the system, threefold anchoring of the  $C_3$ -symmetric macrocycle to  $C_{60}$  by means of a Bingel tris-addition reaction<sup>[14]</sup> was envisaged.<sup>[15,16]</sup> We found that, due to the semirigid nature of the tethers employed, this key reaction proceeded with very high regioselectivity and full diastereoselectivity.<sup>[17]</sup>

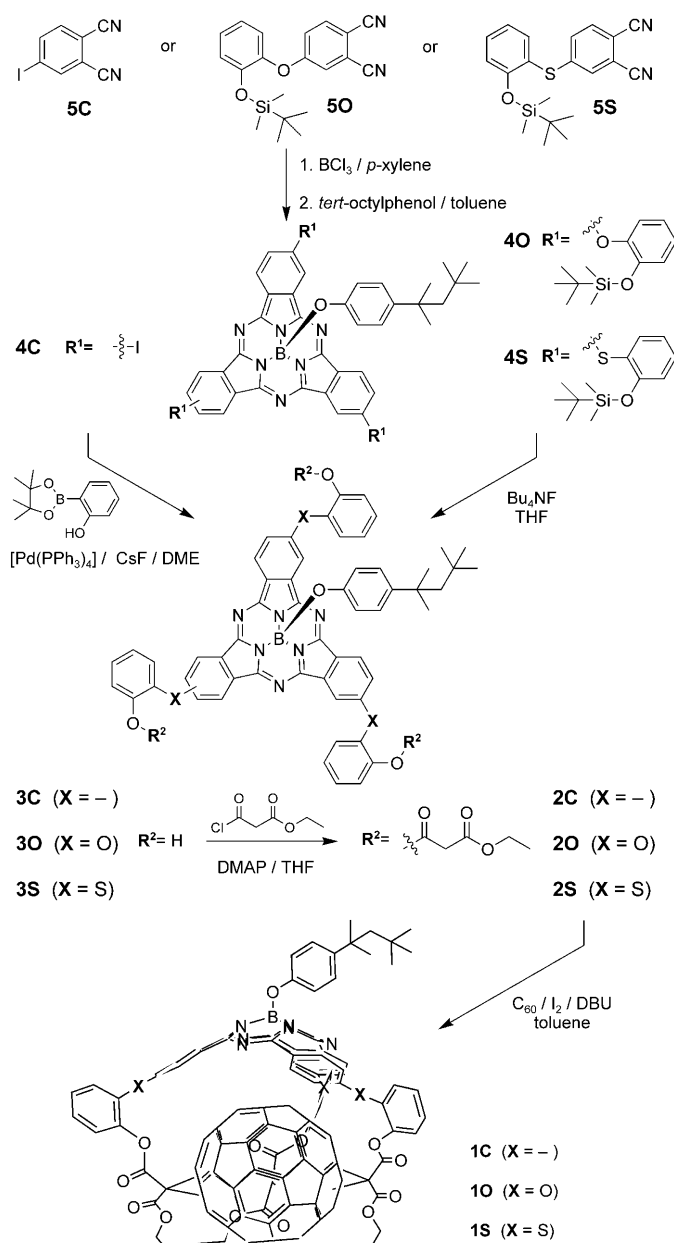
The three SubPc- $C_{60}$  D–A systems prepared (Scheme 1)<sup>[18]</sup> show only small differences in the connection of the spacer to the SubPc macrocycle: a direct C–C bond (C series), an oxygen atom (O series), or a sulfur atom (S series). Analysis of SubPc- $C_{60}$  products **1C**, **1O**, and **1S** by <sup>1</sup>H NMR spectroscopy and HPLC revealed that the regioselectivity of the final tris-addition process is very sensitive to the length and flexibility of the spacer in  $C_3$ -symmetric SubPc precursors **2C**, **2O**, and **2S**. For instance, compound **2O**, having a phenoxy spacer, meets all the requirements for fully regioselective tris-addition to  $C_{60}$  to yield a single regioisomer with  $C_3$  symmetry (**1O**; Figure 1 and Figures S6–S9, Supporting Information). In contrast, the reaction of SubPc **2C** at 20 °C yielded a 5:95 mixture of two regioisomers (**1C $\alpha$**  and **1C $\beta$** ; Figure 1 and Figures S1–S5, Supporting Information) that could be separated by column chromatography. The minor component (**1C $\alpha$** ) clearly retains the original  $C_3$  symmetry of the precursor SubPc, whereas **1C $\beta$**  has  $C_1$  symmetry. The shorter nature of the biphenyl linker seems to restrict formation of a  $C_3$ -symmetric tris-addition product, and the tether prefers to anchor in a less symmetric arrangement to release strain.<sup>[18]</sup> These triple addition reactions are not only highly regioselective, but also totally diastereoselective; each SubPc enantiomer generates only one enantiomeric addition pattern. Such selectivities are lost, however, in the formation of **1S** from SubPc **2S**. Analyses by NMR and HPLC revealed the presence of a complex mixture of isomers that was difficult to separate (Figure S10, Supporting Information). The slightly higher flexibility and diameter of the tether in **2S** must be responsible for this effect.

[\*] Dr. E. Carbonell, Prof. Dr. D. M. Guldi  
Department of Chemistry and Pharmacy and Interdisciplinary  
Center for Molecular Materials (ICMM)  
Friedrich-Alexander-Universität Erlangen-Nürnberg  
Egerlandstrasse 3, 91058 Erlangen (Germany)  
Fax: (+49) 9131-852-8307  
E-mail: dirk.guldi@chemie.uni-erlangen.de

Dr. D. González-Rodríguez, Prof. T. Torres  
Departamento de Química Orgánica (C-I)  
Facultad de Ciencias, Universidad Autónoma de Madrid  
Cantoblanco, 28049 Madrid (Spain)  
Fax: (+34) 91-497-3966  
E-mail: tomas.torres@uam.es  
Homepage: <http://www.uam.es/gruposinv/ftalo/>

[\*\*] Funding from MEC (CTQ2008-00418/BQU, CONSOLIDER-INGENIO 2010 CDS2007-00010 NANOCIENCIA MOLECULAR), ESF-MEC (MAT2006-28180-E, SOHYDS), COST Action D35, and CAM (S-0505/PPQ/000225) is acknowledged. This work was also supported by the Deutsche Forschungsgemeinschaft through SFB583, DFG (GU 517/4-1), FCI, and the Office of Basic Energy Sciences of the U.S. Department of Energy. We would like to acknowledge Dr. Carmen Atienza Castellanos for the electrochemistry studies.

Supporting information for this article is available on the WWW under <http://dx.doi.org/10.1002/anie.200902767>.



**Scheme 1.** Synthesis of SubPc-C<sub>60</sub> dyads **1C**, **1O**, and **1S**. DBU = 1,8-diazabicyclo[5.4.0]undec-7-ene, DMAP = 4-dimethylaminopyridine.

To ascertain the binding patterns to the fullerene in **1C $\alpha$** , **1C $\beta$** , and **1O**, we performed molecular modeling studies using a combination of semiempirical (PM3) and DFT (B3LYP/6-31G) methods.<sup>[18]</sup> Due to the rigid nature of the SubPc core and the restricted flexibility of the spacers, the number of possible tris-addition patterns is quite limited. So, among the four possible C<sub>3</sub>-symmetric tris-addition patterns to C<sub>60</sub> (*c1,c1,c1*, *e,e,e*, *t3,t3,t3*, and *t4,t4,t4*),<sup>[14,19]</sup> only the *t3,t3,t3* isomer can be expected for compounds **1C $\alpha$**  and **1O**, while the other three isomers have rather strained structures (quite obvious for the *c1,c1,c1* and *e,e,e* patterns) due to the smaller spacing between the cyclopropane rings.<sup>[20]</sup> This assignment was further supported by some of the features found in the NMR spectra. For instance, only a *t3,t3,t3* tris-addition pattern

is consistent with the exceptional upfield shift experienced by proton **a** in compound **1O** since, due to the conformation adopted by the spacer, it is affected by the aromatic ring current of the nearby phenyl group (Figure 1). The NOESY and <sup>13</sup>C NMR spectra are also in accordance with this assignment. On the other hand, a *t3,t3,t4* regioisomeric binding pattern was assigned to C<sub>1</sub>-symmetric compound **1C $\beta$** .<sup>[18,21]</sup>

We have therefore in hand two C<sub>3</sub>-symmetric, *t3,t3,t3* SubPc-C<sub>60</sub> tris-adducts (**1C $\alpha$**  and **1O**) that basically differ in the spacing between the two complementary  $\pi$  surfaces, as imposed by the nature of the tether. In fact, the DFT-optimized structures show that, in **1C $\alpha$** , the concave face of the SubPc is kept in tight van der Waals contact (3.25–3.30 Å) with the C<sub>60</sub> sphere (which explains the low yield of this compound), while in compound **1O** the distance increases to 3.5–3.6 Å.<sup>[18,22,23]</sup> We reasoned that these small  $\pi$ - $\pi$  distances in such rigid structures must influence the molecular orbitals and the electronic interaction between the two redox- and photoactive units. This is clearly reflected in ground-state electronic absorption and cyclic voltammetry measurements. For instance, the UV/Vis spectra of **1C $\alpha$**  and **1O** show broadening, a bathochromic shift, and tailing of the SubPc Q band, more significant for **1C $\alpha$** , compared to **2C** and **2O**, respectively (Figure 2a). The features of this transition did not change with changing solvent polarity (i.e., toluene, CHCl<sub>3</sub>, THF, or benzonitrile) or concentration. Similarly, substantial shifts in the redox features of the two electron donor-acceptor conjugates relative to the references indicate appreciable electronic interactions between the active moieties (i.e., electron-donating SubPc and electron-accepting C<sub>60</sub>; see Table 1). In particular, SubPc oxidation reveals the extent of electronic change. For example, the closer SubPc-C<sub>60</sub> separation in **1C $\alpha$**  leads to larger differences in the first oxidation step (190 mV) relative to **1O** (70 mV). Additionally, fullerene reduction becomes appreciably harder, by approximately 60–90 mV.

**Table 1:** Half-wave potentials of the first redox processes and some photo-physical parameters of a reference tris(diethylmalonate)-C<sub>60</sub> (**6**),<sup>[18]</sup> SubPcs **2C** and **2O**, and SubPc-C<sub>60</sub> dyads **1C $\alpha$**  and **1O**.

	Solvent	<b>6</b>	<b>2C</b>	<b>2O</b>	<b>1C<math>\alpha</math></b>	<b>1O</b>
SubPc oxidation <sup>[a]</sup>	THF		+1.03	+1.13	+1.22	+1.20
C <sub>60</sub> reduction <sup>[a]</sup>	THF	−0.54			−0.60	−0.63
$\Phi$ SubPc <sup>[b]</sup>	toluene		0.08		5.8 × 10 <sup>−4</sup>	8.5 × 10 <sup>−4</sup>
	THF		0.081	0.08	5.2 × 10 <sup>−4</sup>	7.3 × 10 <sup>−4</sup>
	benzonitrile		0.079		3.9 × 10 <sup>−4</sup>	6.2 × 10 <sup>−4</sup>
$\Phi$ C <sub>60</sub> <sup>[b]</sup>	toluene					8.0 × 10 <sup>−4</sup>
	THF	8.0 × 10 <sup>−4</sup>				6.2 × 10 <sup>−4</sup>
$\tau$ SubPc <sup>[c]</sup>	THF		1.6	1.7	< 0.1	< 0.1
	THF	1.7				1.7
$k_{\text{singlet}}$ <sup>[d]</sup>	THF				9.5 × 10 <sup>10</sup>	6.7 × 10 <sup>10</sup>

[a] Determined by cyclic voltammetry. Data in Volts versus Ag/Ag<sup>+</sup>. [b] SubPc or C<sub>60</sub> fluorescence yield. [c] SubPc or C<sub>60</sub> fluorescence lifetime [ns]. [d] Singlet-excited-state deactivation rates [s<sup>−1</sup>].

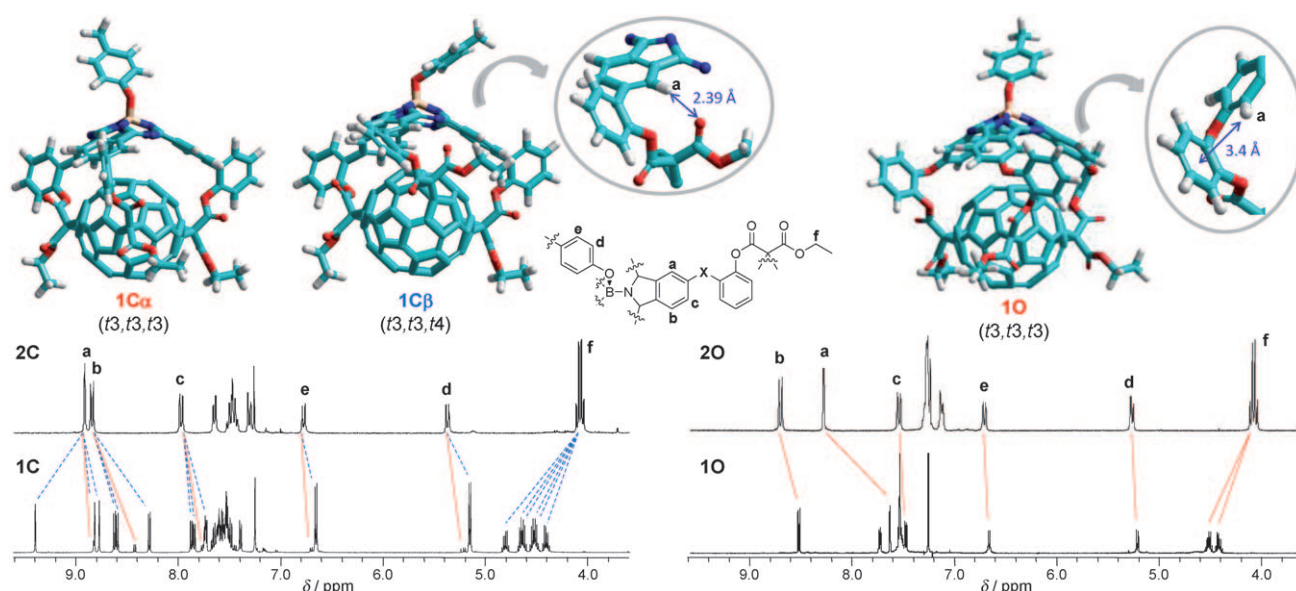


**Figure 1.**  $^1\text{H}$  NMR spectra ( $\text{CDCl}_3$ , 298 K, 500 MHz) of SubPc- $\text{C}_{60}$  dyads **1C** and **1O** compared to those of SubPc precursors **2C** and **2O**. In the case of **1C**, formation of a 5:95 mixture of two isomers **1C $\alpha$**  (one set of signals; solid lines) and **1C $\beta$**  (three sets of signals; dashed lines) was observed. Formation of a 1:1 mixture of two enantiomers is evidenced in the splitting of the diastereotopic methylene protons (**f**) on tris-adduct formation. On top, the optimized structural models of **1C $\alpha$** , **1C $\beta$** , and **1O** are shown, together with a magnification showing the conformation of the spacers in **1C $\beta$**  and **1O**, which may explain the extraordinary downfield (for **1C $\beta$** )<sup>[21]</sup> or upfield (for **1O**) shift of the signal of proton **a**.

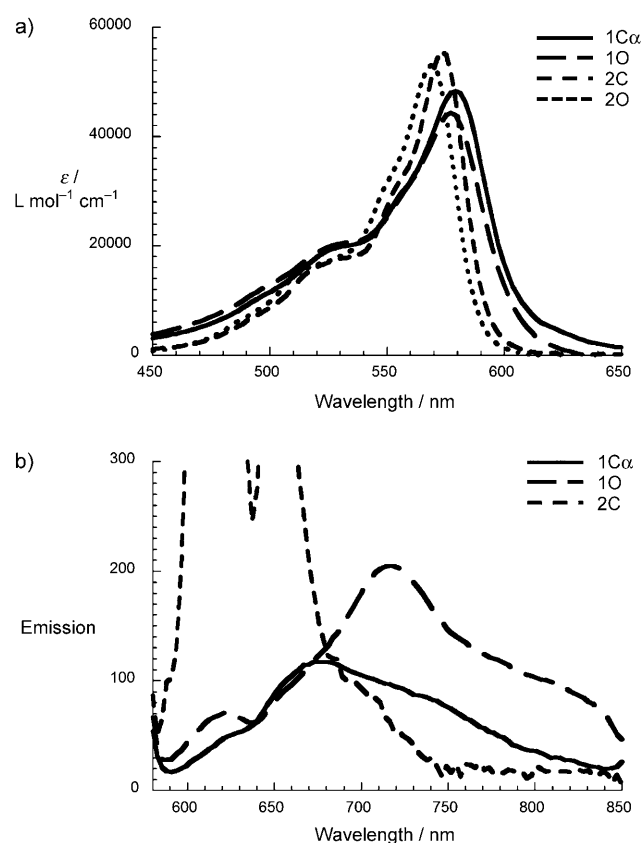


**Figure 2.** a) Electronic absorption spectra ( $\text{CHCl}_3$ ,  $c = 10^{-5} \text{ M}$ ) of SubPc- $\text{C}_{60}$  dyads **1C $\alpha$**  and **1O** compared to those of SubPcs **2C** and **2O**. b) Steady-state fluorescence spectra of **2C** (attenuated by a factor of 10), **1O**, and **1C $\alpha$**  in toluene solutions exhibiting the same absorption of 0.1 at the excitation wavelength of 560 nm. See also Figure S16 (Supporting Information).

When comparing the fluorescence spectra of **1C $\alpha$ /1O** with those of **2C/2O**, strong SubPc fluorescence quenching becomes evident (see Table 1).<sup>[24]</sup> A closer analysis of the fluorescence spectra for **1O** reveals, besides the strongly quenched SubPc fluorescence in the 580–650 nm range, the familiar  $\text{C}_{60}$  fluorescence in the red (i.e., 650–850 nm; Figure 2b). The  $\text{C}_{60}$  fluorescence quantum yields, which are about  $(8.0 \pm 0.2) \times 10^{-4}$  in toluene, THF, and benzonitrile, suggest quantitative transduction of singlet-excited-state energy from SubPc (i.e., 2.0 eV) to  $\text{C}_{60}$  (i.e., ca. 1.7 eV).<sup>[25]</sup> On the contrary, for **1C $\alpha$** , the lack of  $\text{C}_{60}$  fluorescence implies a different reactivity, namely, charge separation to form the one-electron-reduced  $\text{C}_{60}$  radical anion and the one-electron-oxidized SubPc radical cation (see below).

Transient absorption measurements shed light onto the photoreactivity of **2C/2O** and **1C $\alpha$ /1O**. On 550 nm excitation of **2C/2O** we observed the singlet-excited-state characteristics of SubPc (Figure S17, Supporting Information). In both cases, bleaching of the ground state dominates the transient absorption spectrum, accompanied by a new transition that develops in the red. For **2C/2O**, maxima and minima evolve around 460, 635, and 560 nm, respectively. The rate of intersystem crossing converting the strongly emitting singlet excited state to the corresponding triplet manifold is  $(6.3 \pm 0.2) \times 10^8 \text{ s}^{-1}$ . In the nanosecond regime the triplet features, which involve transient bleaching of the ground-state maximum and a broad transient maximum between 600 and 900 nm, are monitored.<sup>[12a]</sup> The triplet lifetimes in deoxygenated THF are 28  $\mu\text{s}$  and involve quantitative recovery of the singlet ground state.

The photoreactivity of **1O** is different from those of **2C** and **2O**, although on the nanosecond timescale the only detectable product is the long-lived SubPc triplet excited state

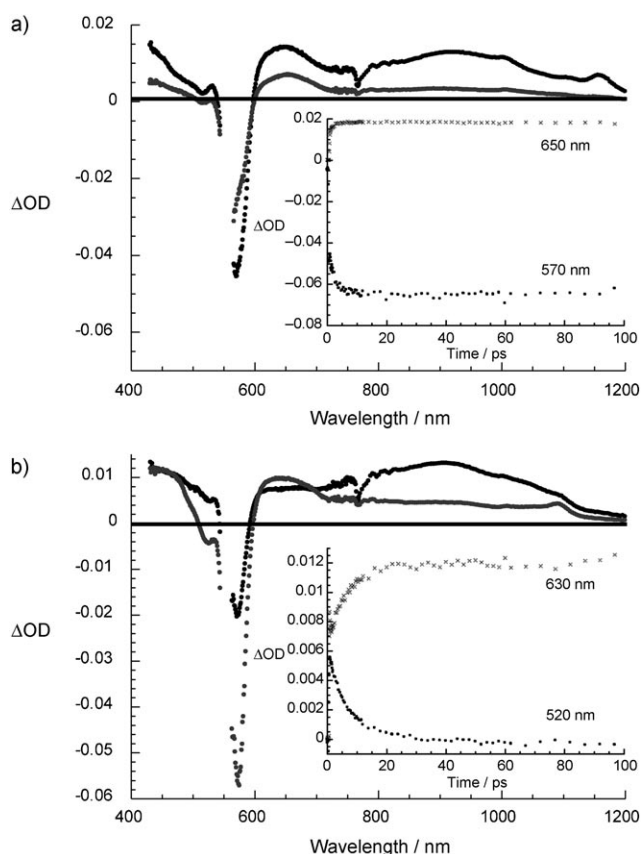


**Figure 3.** Differential absorption spectra (visible and near-infrared) obtained on femtosecond flash photolysis (550 nm, 150 nJ) of **1O**/**1Cα** in THF with several time delays between 0 (black line) and 3000 ps (gray line) at room temperature. a) **1O**. Inset: time-absorption profiles of the spectra at 570 and 650 nm, monitoring the decay of the SubPc singlet excited state. b) **1Cα**. Inset: time-absorption profiles of the spectra at 520 and 630 nm, monitoring the decay of the SubPc singlet excited state and formation of the radical-ion pair state. See also Figure S18 (Supporting Information).

(1.45 eV). The mechanism for converting the initially formed SubPc singlet excited state (see Figure 3a) into the final SubPc triplet excited state differs from that seen in **2C** and **2O**: It is a cascade of energy-transfer processes with rate constants of  $1.5 \times 10^{11} \text{ s}^{-1}$  (i.e., singlet–singlet energy transfer),  $6.3 \times 10^8 \text{ s}^{-1}$  (i.e., intersystem crossing), and  $\gg 6.3 \times 10^8 \text{ s}^{-1}$  (i.e., triplet–triplet energy transfer). Similar reactivity was reported for several weakly coupled SubPc–C<sub>60</sub> conjugates, in which the SubPc, unless substituted with strongly electron-donating groups (i.e., amines), usually behaved as an excited-state energy donor.<sup>[12a,d]</sup>

The transient absorption changes monitored for **1Cα** are substantially different from the aforementioned cases (i.e., **2C/2O** and **1O**; cf. Figure 3a and b). The visible part, that is, peaks at 440 and 625 nm, which evolve as the initially formed SubPc singlet excited state with maxima and minima at 460, 645 and 560 nm, respectively, transforms into the signals of a new photoproduct. In the visible part, this photoproduct resembles the features known for the one-electron-oxidized SubPc radical cation.<sup>[12a,d]</sup> In the near-infrared part, on the other hand, the characteristic fingerprint of the one-electron

reduced C<sub>60</sub> radical anion around 1090 nm is seen.<sup>[26]</sup> This confirms formation of the SubPc<sup>•+</sup>–C<sub>60</sub><sup>•–</sup> radical-ion pair. From the time-absorption profiles a charge-separation rate constant of  $1.4 \times 10^{11} \text{ s}^{-1}$  was derived in THF, which is in good agreement with the steady-state fluorescence experiments. As Figure 3b demonstrates, the SubPc<sup>•+</sup>–C<sub>60</sub><sup>•–</sup> pair is surprisingly stable on our femtosecond timescale (i.e., up to 1500 ps) and starts to decay on the nanosecond timescale (i.e., starting at 8 ns). In THF, a lifetime of 97 ns ( $1.0 \times 10^7 \text{ s}^{-1}$ ) was found. A likely explanation for this remarkably long-lived charge-transfer state may be—besides the low reorganization energies of C<sub>60</sub> and SubPc—stabilization of the SubPc<sup>•+</sup> species by partial charge shift to the axial electron-rich phenoxy group.<sup>[27]</sup>

Our results shed light on the role of electron donor–acceptor spacing and orbital overlap on the subtle interplay between photoinduced energy- and charge-transfer mechanisms. The main attributes of our capped SubPc–C<sub>60</sub> systems, compared to similar systems studied previously,<sup>[15,16]</sup> are: 1) the low conformational flexibility owing to threefold tethering with rigid spacers, 2) a high degree of orbital overlap due to the complementarity of the  $\pi$  surfaces, and 3) the possibility of tailoring the distance between electron donor and acceptor. Remarkably, the short SubPc–C<sub>60</sub> distance and high orbital overlap in **1Cα** leads to notable perturbation of the electronic structure of both components in the ground state, as evidenced, for example, in the absorption spectra and redox potentials. A reasonable rationale implies a partial shift of electron transfer density. In this pre-activated state, charge separation is favored over energy transfer. In the case of slightly larger interchromophore distances and/or higher flexibility, as in **1O**, weaker ground-state interactions result in dominant energy-transfer deactivation, despite the similar HOMO(SubPc)–LUMO(C<sub>60</sub>) gap (ca. 1.82 eV;<sup>[28]</sup> see Figure S15, Supporting Information) of both systems.

Received: May 24, 2009

Revised: July 21, 2009

Published online: September 18, 2009

**Keywords:** electron transfer · energy transfer · fullerenes · subphthalocyanines ·  $\pi$  interactions

- [1] *Handbook of Organic Electronics and Photonics* (Ed.: H. S. Nalwa), American Scientific Publishers, New York, **2008**.
- [2] S. Guenes, H. Neugebauer, N. S. Sariciftci, *Chem. Rev.* **2007**, *107*, 1324–1338.
- [3] *Molecular Mechanisms of Photosynthesis* (Ed.: R. E. Blankenship), Blackwell, Oxford, **2002**.
- [4] H. Imahori, H. Yamada, D. M. Guldi, Y. Endo, A. Shimomura, S. Kundu, K. Yamada, T. Okada, Y. Sakata, S. Fukuzumi, *Angew. Chem.* **2002**, *114*, 2450–2453; *Angew. Chem. Int. Ed.* **2002**, *41*, 2344–2347.
- [5] Y. Araki, O. Ito, *J. Photochem. Photobiol. C* **2008**, *9*, 93–110.
- [6] D. M. Guldi, A. Hirsch, M. Scheloske, E. Dietel, A. Troisi, F. Zerbetto, M. Prato, *Chem. Eur. J.* **2003**, *9*, 4968–4979.
- [7] B. Albinsson, M. P. Eng, K. Pettersson, M. U. Winters, *Phys. Chem. Chem. Phys.* **2007**, *9*, 5847–5864.
- [8] A. Harriman, *Angew. Chem.* **2004**, *116*, 5093–5095; *Angew. Chem. Int. Ed.* **2004**, *43*, 4985–4987.



- [9] G. Feher, J. P. Allen, M. Y. Okamura, D. C. Rees, *Nature* **1989**, 339, 111–114.
- [10] a) D. Veldman, S. M. A. Chopin, S. C. J. Meskers, M. M. Groeneveld, R. M. Williams, R. A. J. Janssen, *J. Phys. Chem. A* **2008**, 112, 5846–5857; b) J. M. Giaimo, J. V. Lockard, L. E. Sinks, A. M. Scott, T. M. Wilson, M. R. Wasielewski, *J. Phys. Chem. A* **2008**, 112, 2322–2330.
- [11] a) C. G. Claessens, D. González-Rodríguez, T. Torres, *Chem. Rev.* **2002**, 102, 835–853; b) T. Torres, *Angew. Chem.* **2006**, 118, 2900–2903; *Angew. Chem. Int. Ed.* **2006**, 45, 2834–2837.
- [12] SubPcs have been employed as energy donors,<sup>[12a,d]</sup> electron donors,<sup>[12a,d]</sup> and electron acceptors.<sup>[12b,c]</sup> a) D. González-Rodríguez, T. Torres, D. M. Guldi, J. Rivera, M. A. Herranz, L. Echegoyen, *J. Am. Chem. Soc.* **2004**, 126, 6301–6313; b) D. González-Rodríguez, C. G. Claessens, T. Torres, S.-G. Liu, L. Echegoyen, N. Vila, S. Nonell, *Chem. Eur. J.* **2005**, 11, 3881–3893; c) D. González-Rodríguez, T. Torres, M. M. Olmstead, J. Rivera, M. A. Herranz, L. Echegoyen, C. Atienza-Castellanos, D. M. Guldi, *J. Am. Chem. Soc.* **2006**, 128, 10680–10681; d) D. González-Rodríguez, T. Torres, M. A. Herranz, L. Echegoyen, E. Carbonell, D. M. Guldi, *Chem. Eur. J.* **2008**, 14, 7670–7679.
- [13] C. G. Claessens, T. Torres, *Chem. Commun.* **2004**, 1298–1299.
- [14] For recent reviews on multiple additions to fullerenes, see: a) C. Thilgen, S. Sergeyev, F. Diederich, *Top. Curr. Chem.* **2004**, 248, 1–61; b) A. Hirsch, *Chem. Rec.* **2005**, 5, 196–208; c) Z. Zhou, S. R. Wilson, *Curr. Org. Chem.* **2005**, 9, 789–811.
- [15] Porphyrin–C<sub>60</sub> systems connected through a double tether have been studied. See reference [6] and a) N. Armaroli, G. Marconi, L. Echegoyen, J.-P. Bourgeois, F. Diederich, *Chem. Eur. J.* **2000**, 6, 1629–1645; b) D. M. Guldi, C. Luo, M. Prato, A. Troisi, F. Zerbetto, M. Scheloske, E. Dietel, W. Bauer, A. Hirsch, *J. Am. Chem. Soc.* **2001**, 123, 9166–9167.
- [16] Phthalocyanine–C<sub>60</sub> systems connected through a double tether have also been studied: M. Niemi, N. V. Tkachenko, A. Efimov, H. K. Ohkubo, S. Fukuzumi, H. Lemmetyinen, *J. Phys. Chem. A* **2008**, 112, 6884–6892.
- [17] a) G. Rapenne, J. Crassous, A. Collet, L. Echegoyen, F. Diederich, *Chem. Commun.* **1999**, 1121–1122; b) U. Reuther, T. Brandmüller, W. Donaubauer, F. Hampel, A. Hirsch, *Chem. Eur. J.* **2002**, 8, 2261–2273; c) N. Chronakis, A. Hirsch, *Chem. Commun.* **2005**, 3709–3711.
- [18] See Supporting Information for further details.
- [19] For the sake of simplicity and clarity, we use the terminology: *c* for *cis*, *e* for *equatorial*, and *t* for *trans*: L. Pasimeni, A. Hirsch, I. Lamparth, M. Maggini, M. Prato, *J. Am. Chem. Soc.* **1997**, 119, 12902–12905.
- [20] The formation of the *t4,t4,t4* tris-addition pattern is, moreover, highly electronically unfavorable: S.-C. Chuang, S. I. Khan, Y. Rubin, *Org. Lett.* **2006**, 8, 6075–6078.
- [21] A *t3,t3,t4* regioisomer can impose a different conformation on one of the biphenyl moieties in which a carbonyl group of the malonate moiety is close to the **a** proton of one of the isoindole units, which would explain the unusual downfield shift (> 0.5 ppm) of the proton signal around 9.4 ppm (see Figure 1 and Supporting Information).
- [22] The benzene dimer in its parallel-displaced configuration is held at a distance of 3.6 Å. See, for instance: T. Sato, T. Tsuneda, K. J. Hirao, *J. Chem. Phys.* **2005**, 123, 104307.
- [23] Distances as short as 3.1–3.4 Å have been observed in fullerene host–guest complexes: a) A. Sygula, F. R. Fronczek, R. Sygula, P. W. Rabideau, M. M. Olmstead, *J. Am. Chem. Soc.* **2007**, 129, 3842–3843; b) E. M. Pérez, M. Sierra, L. Sánchez, M. R. Torres, R. Viruela, P. M. Viruela, E. Ortí, N. Martín, *Angew. Chem.* **2007**, 119, 1879–1883; *Angew. Chem. Int. Ed.* **2007**, 46, 1847–1851; c) G. Fernández, E. M. Pérez, L. Sánchez, N. Martín, *Angew. Chem.* **2008**, 120, 1110–1113; *Angew. Chem. Int. Ed.* **2008**, 47, 1094–1097; d) E. M. Pérez, A. L. Capodilupo, G. Fernández, L. Sánchez, P. M. Viruela, R. Viruela, E. Ortí, M. Bietti, N. Martín, *Chem. Commun.* **2008**, 4567–4569; e) E. M. Pérez, N. Martín, *Chem. Soc. Rev.* **2008**, 37, 1512–1519; f) S. Gayathri, M. Wielopolski, E. M. Pérez, G. Fernández, L. Sánchez, R. Viruela, E. Ortí, D. M. Guldi, N. Martín, *Angew. Chem.* **2009**, 121, 829–834; *Angew. Chem. Int. Ed.* **2009**, 48, 815–819.
- [24] The corresponding rate constants of SubPc singlet excited-state deactivation are  $9.5 \times 10^{10} \text{ s}^{-1}$  (**1Ca**) and  $6.7 \times 10^{10} \text{ s}^{-1}$  (**1O**) in THF.
- [25] In fluorescence lifetime measurements a lifetime of 1.7 ns was registered for C<sub>60</sub> fluorescence.
- [26] D. M. Guldi, M. Prato, *Acc. Chem. Res.* **2000**, 33, 695–703.
- [27] In fact, DFT calculations localize the phenoxyl HOMO very close in energy to the SubPc HOMO (see Figure S15, Supporting Information).
- [28] Calculated as the sum of the absolute values of the first oxidation potentials of the SubPc and the first reduction potentials of C<sub>60</sub> (see Table 1).